Journal of Building Engineering 97 (2024) 110837

Contents lists available at ScienceDirect

Journal of Building Engineering

journal homepage: www.elsevier.com/locate/jobe

# Human exposure to respiratory aerosols: Impact of ventilation rates, mixing ventilation configuration, and breathing patterns

Ihab Jabbar Al-Rikabi [a,*], Hayder Alsaad [a], Svenja Carrigan [b], Conrad Voelker [a]

[a] Bauhaus-University Weimar, Department of Building Physics, Weimar, Germany
[b] University of Kaiserslautern-Landau, Department of Building Physics, Kaiserslautern, Germany

ARTICLE INFO

*Keywords:*
Airborne transmission
Cross-infection
Breathing pattern
Air distribution
Ventilation

ABSTRACT

This study investigates airborne transmission dynamics between occupants in office rooms equipped with mixing ventilation (MV). The primary aim was to assess how different ventilation configurations, air change rates (ACH), breathing patterns, and supply air temperatures influence cross-exposure and infection risks. The experimental setup involved two thermal manikins simulating an infected and an exposed occupant within a climate chamber. The investigated parameters included four ACH levels (1.2, 2, 4 and 6.6 $h^{-1}$, representing four EN 16798–1 ventilation categories), two MV configurations (near-ceiling and near-floor inlets), two breathing patterns (nose and mouth breathing), and two supply air temperatures (19 °C and 21 °C). Carbon dioxide ($CO_2$) was used as a tracer gas to simulate exhaled aerosols, enabling precise measurements of effectiveness ($\varepsilon_v$), intake fraction (*IF*), and infection probability (*P*). The findings indicate that higher ACH do not uniformly improve $\varepsilon_v$ but are linked to reduced cross-exposure risk. The near-floor inlet MV configuration significantly outperformed the near-ceiling configuration in reducing *IF* and *P* by 15–41 % under most investigated scenarios. Additionally, mouth breathing increased *IF* and *P* compared to nose breathing, especially at higher ACH (2, 4, and 6.6 $h^{-1}$). The results also showed that lower supply temperatures do not always correlate with higher *IF* and *P*, as MV configuration and breathing patterns significantly influence outcomes. This research provides insights into optimizing ventilation strategies for safer indoor environments, emphasizing the importance of airflow dynamics, breathing patterns, and supply temperature in ventilation design.

**Acronyms**

| | |
|---|---|
| ACH | Air change per hour |
| BZ | Breathing zone |
| CRE | Contaminant removal effectiveness |
| $CO_2$ | Carbon dioxide |
| $C_a$ | Concentration at any of inside the room |
| $C_{bkg}$ | Background concentration of the room before dosing from the infected manikin |
| $C_e$ | Concentration at exhaust of the room |
| $C_{exp}$ | Concentration at the breathing zone of the exposed occupant |

* Corresponding author. Coudraystraße 11a, 99423, Weimar, Germany.
*E-mail address:* ihab.al-rikabi@uni-weimar.de (I.J. Al-Rikabi).

https://doi.org/10.1016/j.jobe.2024.110837
Received 26 July 2024; Received in revised form 19 September 2024; Accepted 21 September 2024
Available online 22 September 2024

| | |
|---|---|
| $C_s$ | Concentration at supply of the room |
| $C_{inf}$ | Concentration at the exhalation of the infected manikin |
| $D$ | Dilution ratio |
| $\varepsilon_e$ | Personal exposure indices |
| $\varepsilon_v$ | Ventilation effectiveness |
| IAQ | Indoor air quality |
| $IF$ | Intake fraction |
| MV | Mixing ventilation |
| NC | Near-ceiling |
| NF | Near-floor |
| $P$ | Probability of infection |
| $I$ | Number of infectors |
| $q$ | Quanta emission rate |
| $p$ | Breathing rate of healthy occupants |
| $Q$ | Space ventilation rate |

## 1. Introduction

Individuals typically spend 80–90 % of their time within indoor environments, which are often characterized by limited space and variable levels of ventilation. Such conditions can potentially elevate the risk of airborne transmission, making these environments critical areas of focus for understanding and mitigating disease spread [1]. Therefore, effective and thoughtfully designed ventilation systems are crucial for maintaining a high indoor air quality (IAQ). Factors such as airflow dynamics, type of mixing ventilation configuration, and air change per hour (ACH) play a vital role in this context [2]. The intricate interplay between these factors is paramount for occupant well-being and productivity [2]. Moreover, by optimizing these systems for efficiency, there is a significant opportunity to enhance IAQ while simultaneously reducing energy consumption. This dual benefit underscores the importance of innovative approaches in ventilation system design [3].

In indoor environments, airborne cross-infection between an infected individual and an exposed person occurs through direct and indirect transmission routes [4]. Direct transmission arises when the exhaled air of the infected individual is inhaled by the exposed person after entering and commingling with the exposed person's breathing zone air. In contrast, indirect transmission occurs when the exhaled air from the infected person diffuses and blends with the room air prior to reaching the breathing zone, subsequently being inhaled by the exposed person. The risk of cross-infection through direct transmission is subject to several variable parameters, including air distribution, the spatial separation between individuals, their positions and orientations, respiratory patterns, activity levels, and occupant mobility. Conversely, the risk of cross-infection via indirect transmission primarily hinges on the occupied space's volume and the rate of the ventilation supply airflow [5].

Mixing ventilation (MV) is the most widely-used mechanical system in both literature and practice, particularly in office spaces, owing to its versatility and effectiveness in achieving thermal comfort [6]. The widespread utilization of MV systems can be attributed to their ability to maintain uniform conditions throughout enclosed spaces, fostering a homogenous distribution of temperature and air quality parameters [7]. Several factors directly affect MV's performance on IAQ, such as supply flow rates, location of MV air terminals, indoor heat sources including the human thermal plume, and breathing pattern [8–12]. Ye et al. [11] reported that increasing the supply air flow rate of an MV system effectively mitigated the background aerosol concentration while it had a limited effect on the local concentration. Yet, other studies reported that increasing the supply flow rate for MV might not always be proportional to reducing the concentration of contaminants [8,11,13–15]. The location of MV ventilation air terminals can also affect the IAQ. However, the literature shows only a limited number of studies in this regard. For example, Licina et al. [16] reported that airflows originating from the front and the side exhibit greater efficacy in reducing exposure risk than airflow operating from above (ceiling supply). Additionally, Berlanga et al. [17] experimentally studied four MV configurations (wall grill, swirl diffuser, low-exhaust, and high-exhaust) on exposure risk in a hospital ward. Their study reported that a swirl diffuser achieved lower exposure risk than other MV configurations. Further studies illustrated that the location of supply air terminals could impact the dilution of contaminants, and the proximity of supply inlets to infected occupants results in enhanced air dilution around the infected, thereby reducing the transmission of aerosols [13,18–20]. Nevertheless, it has been demonstrated that high supply air flow rates might increase the diffusion of aerosols, contingent upon the positioning of supply terminals [13,15,21]. Thus, defining an optimal supply flow rate contingent upon the spatial arrangement of the MV air terminals becomes imperative.

Another crucial parameter that could influence the distribution of airborne contaminants within the occupants' microenvironment is the indoor air temperature [22]. This plays a crucial role in the development of the human body convective boundary layer and the thermal plume; a higher temperature differential between the human body and the ambient environment correlates with an increased expansion of the convective flow in the microenvironment encasing the body [23]. Consequently, the growth of the convective flow can carry or transport more contaminants. For example, Ai et al. [8] reported that the cross-exposure risk between two standing occupants exhibited a lower magnitude at a lower indoor temperature (22 °C) in comparison to higher indoor temperatures (23 °C and 24 °C). Additionally, in environments where the indoor air movement is minimal (as in MV system), the thermal plume generated by humans becomes the predominant airflow within the immediate surroundings of an individual. For example, Zhong et al. [24] reported

that for a thermal manikin, it was observed that the direct exposure to particulate matter was increased by 200 % in comparison to non-thermal manikin (unheated manikins), whereas the indirect exposure reduced by 60 %. Consequently, the total exposure experienced a 69 % increase in comparison to scenarios using non-thermal manikin (unheated manikins).

Similar to the convective airflow in the vicinity of the human body, the flow around indoor heat sources located near the occupants can have a large impact on the cross-transmission of airborne contaminants between occupants. The literature reports that the presence of heat sources near the infected or exposed occupant can substantially impact the exposure risk [9,25]. Peng et al. [25] conducted experimental inquiries into the impact of heat sources (table lamps) on contaminants removal effectiveness (CRE) between two manikins within a 37.8 $m^3$ climate chamber. Their investigation revealed that under active source conditions (with heat), the CRE was approximately 1.3, whereas under passive source conditions (without heat), it ranged between 0.68 and 0.82. Xie et al. [9] conducted a numerical exploration into the impact of heat sources on airborne exposure between two occupants within a 38.4 $m^3$ room. Their findings revealed that the average inhaled contaminants and infection risk in the presence of heat sources were approximately 2 and 1.79 times higher, respectively, compared to scenarios without heat sources. Therefore, excluding the heat sources while evaluating the exposure to respiratory aerosols could give unrealistic results.

In addition to air convection surrounding the human body and other indoor heat sources, the breathing pattern can also largely influence the potential for cross-infection via direct transmission. For example, Villafruela et al. [26] numerically studied the effect of breathing patterns (mouth breathing and nose breathing) on the exposure to airborne contaminants between two standing occupants. Their study reported that the breathing pattern can significantly impact the microenvironment around the occupant. Liu et al. [22] experimentally investigated the transmission of respiratory droplets over short distances using two breathing manikins. Their study reported that at short spreading distance of 0.8 m between the two manikins, the exposure risk under mouth breathing was about 2.4 times higher compared to nose breathing. Qian et al. [27] experimentally investigated the impact of mouth and nose breathing on IAQ in a two-bed hospital ward equipped with MV. Their findings revealed comparable personal exposure indices ($\varepsilon_e$) under both mouth and nose breathing conditions when the bed separation distance was 1 m. However, at reduced separation distances (0.5 m), mouth breathing exhibited a 7 % higher $\varepsilon_e$ compared to nose breathing.

The above-mentioned studies highlight the impact of the different parameters on the performance of MV. However, there are several gaps in the literature [28]. An important gap is that most previous studies on the effect of the location of MV air terminals on IAQ were conducted in hospital wards [20,30]; there is a lack of studies on the effect of locations of MV supply inlets and breathing patterns on cross-exposure to respiratory aerosols in an office environment [31]. Additionally, some previous studies evaluated the effect of MV configuration on exposure to contaminants under a fixed flow rate [19] or assessed the influence of air flow rate and ventilation patterns exclusively concerning cross-exposure risk, sometimes with the absence of heat sources near the occupants [4,8]. Moreover, numerous previous studies on respiratory aerosol exposure have utilized heated dummies, which do not adequately mimic the complex intricacies of the human body, unlike thermal manikins. Heated dummies, often designed with simplistic rectangular or circular shapes, fall short in capturing the detailed thermal and geometric characteristics essential for an accurate assessment of cross-exposure risks. This limitation underscores the need for employing thermal manikins that more realistically represent human body dynamics in aerosol dispersion studies. It is imperative to note that the geometric characteristics of the human body significantly influence the convective boundary layer and thermal plume dynamics, consequently impacting the assessment of cross-exposure risks. Thus, utilizing heated dummies may overlook critical nuances inherent in human physiology, potentially leading to inaccuracies in risk assessment associated with airborne transmission [12,24,29]. Further, when investigating the effects of the breathing pattern, the existing literature often focuses on standing or lying positions, primarily concentrating on short distances ($\geq$1 m). There is a lack of studies that focus on the impact of breathing patterns in seated positions, particularly at greater separation distances, especially within configurations that replicate real office environments.

To address these gaps, the current study aims to empirically examine the cross-exposure and infection risk between occupants in an office setup; the experiments were carried out in a controlled climate chamber using two thermal manikins. The emphasis of the study was placed on (a) the effect of ACH on the IAQ, (b) the influence of supply location for MV on the spread of exhaled aerosols between occupants, (c) the effect of breathing patterns on exposure to the exhaled contaminants between occupants, and (d) the effect of supply temperature on IAQ.

## 2. Methodology

### 2.1. Experimental apparatus and setup

The experiments took place in the climate chamber of the Department of Building Physics at the Bauhaus-University Weimar. This chamber, measuring 3 × 3 × 2.44 m, is a room-in-room construction enclosed within a laboratory hall to ensure isolation from the outdoor environmental conditions. It comprises insulated sandwich panels with a heat transfer coefficient of U = 0.27 W/$m^2$·K, offering high thermal insulation from the laboratory hall. The interior surfaces of the chamber are equipped with water-bearing capillary tubing positioned below the floor tiles and the gypsum plaster of the walls and ceiling. Thus, the temperature within the chamber is controllable through the temperature regulation of each interior surface separately. However, in this study this system was switched off. The chamber is equipped with a mixing ventilation system that employs two supply air inlets to introduce fresh or recirculated air at an adjustable flow rate into the chamber (see also Fig. 2 (a)). The air inlets are positioned at one of the corners of the chamber; each inlet comprises a set of six pipes with a diameter of 0.045 m. Simultaneously, the chamber employs two exhaust air outlets with dimensions and characteristics identical to those of the inlets. These outlets are situated at the opposite corner of the inlets. Each inlet and outlet duct are equipped with a valve to regulate the aperture percentage or to entirely close the duct. The ventilation system of the climate chamber offers five different ventilation rates (27.2, 43.9, 62.2, 89.6, and 146 $m^3$/h), corresponding to ACH of 1.2, 2, 2.8, 4,

and 6.6 $h^{-1}$, respectively. In this study, the temperature of the chamber is controlled by the supply temperature of the ventilation system. However, due to internal loads the air temperature is higher especially at low ventilation rates.

To replicate an office environment, an office setup was arranged in the climate chamber with two thermal manikins with complex male body shape (1.76 m tall in the standing position) (Figs. 1 and 2a). The manikins were seated face-to-face given this position's prevalence in office environments. Previous research has indicated that this specific seating configuration exhibits a higher infection risk than face-to-back or side-to-side sitting positions [30–33]. The separation distance between the nose tips of the two manikins was 1.3 m, which has been employed in prior research investigations replicating office environments [34,35]. Each thermal manikin faced a PC monitor with dimensions of 0.34 m (height) × 0.45 m (length) × 0.03 m (width), common for PC screens in office settings; each monitor was connected to a PC workstation measuring 0.4 m × 0.18 m × 0.4 m and placed below the desk. Both manikins were operated using the so-called comfort mode, which simulates the heat generation from a seated calm occupant. This mode was selected for this study as it is widely used in the literature [36–38]. As the measurements are also intended to validate future numerical models, the manikins were seated on open chair frames without clothing or hair to simplify the geometric modelling [39,40].

To study cross-exposure, the first manikin simulated an exposed person; this manikin has 22 body segments. The breathing system of the exposed manikin was switched off, as it has been shown in the literature that the breathing patterns of a healthy occupant have a negligible impact on the assessment of exposure levels [41]. The second manikin simulated an infected person; this manikin has 28 body segments and is equipped with artificial lungs (air pumps with a capacity of 73 L/min) to replicate the respiration process. These lungs can be connected to either the nostrils or the mouth of the manikin, allowing flexible control of the breathing pattern (Fig. 2 (c)). The breathing system of the infected occupant was set to continuous isothermal breathing with a pulmonary ventilation rate of 6.4 L/min [36]. This was selected because the literature indicates that the infected occupant's sinusoidal breathing pattern has a negligible impact on assessing exposure levels compared to continuous breathing [41]. The nostrils feature circular openings, each with a cross-sectional area of 50 $mm^2$. The two jets from the nostrils were oriented at a 30° angle from each other and inclined at a 45° downward angle from the horizontal plane; the mouth featured a 100 $mm^2$ ellipsoidal opening. Thus, the characteristics of nostrils and mouth align with the descriptions provided in the literature [42,43].

### 2.2. Quantified parameters and instrumentation

Carbon dioxide ($CO_2$) was selected as a tracer gas to simulate virus-laden droplet nuclei exhaled by the infected manikin. Noteworthy distinctions exist between tracer gases and airborne particles; particles undergo loss from air streams due to deposition and filtration processes, while the tracer gases do not partake in analogous physical mechanisms. This deviation in behavior necessitated an in-depth exploration of transport dynamics and ramifications for indoor air quality. Numerous investigations have investigated the differences between indoor airborne particles and tracer gases in the context of person-to-person exposure, highlighting the use of tracer gas for investigating cross-exposure risks during non-violent respiratory activities such as breathing and speaking [44–46]. Furthermore, prevailing particle sizes during breathing predominantly fall below 1 μm [47]. Consequently, in this study, $CO_2$ served as the tracer gas to examine person-to-person exposure risks, aligning with the previous studies.

Throughout the experiments, $CO_2$ was introduced at a flow rate of 3 mL/s into a mixer box connected to the exhalation tubing of the infected manikin, as illustrated in Fig. 2 (c). The dosing was conducted using an INNOVA multichannel sampling and monitoring system to ensure precise control of the introduced tracer gas into the mixer box. Two distinct instruments were employed for measuring the $CO_2$ concentration: ALMEMO $CO_2$ sensors and the INNOVA monitor. The $CO_2$ sensors were used to measure the $CO_2$ concentration within the breathing zone (BZ) of the exposed occupant ($C_{exp}$), which was measured at a distance of 0.5 cm from the mouth [43]. These sensors detect $CO_2$ concentrations from 0 to 5000 ppm using the non-dispersive infrared (NDIR) principle with a 2-beam infrared measuring cell. The air pressure dependence of the $CO_2$ measurement is compensated by a built-in air pressure sensor element. The $CO_2$ sensor exhibited an accuracy of ±50.0 ppm; the response time of this sensor is around 1 min for instantaneous values. On the other hand, the INNOVA monitor was used to measure the $CO_2$ at five locations: the concentration in the supply inlet ($C_s$), the concentration in the exhaust outlet ($C_e$), the exhaled concentration from the infected manikin ($C_{inf}$) (as shown in Fig. 2 (c)), and the concentration at two control points in the room (marked as P1 and P2 in Figs. 1 and 2 (a) & (b)). These points were located close to each manikin,

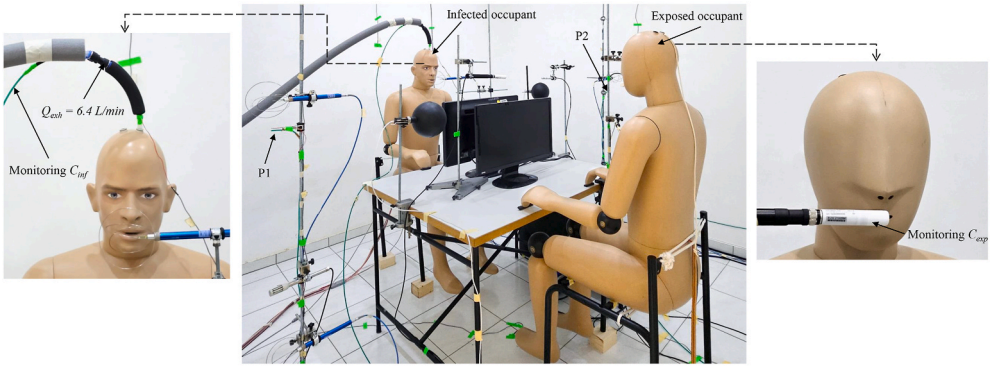


**Fig. 1.** The experimental setup in the climate chamber.

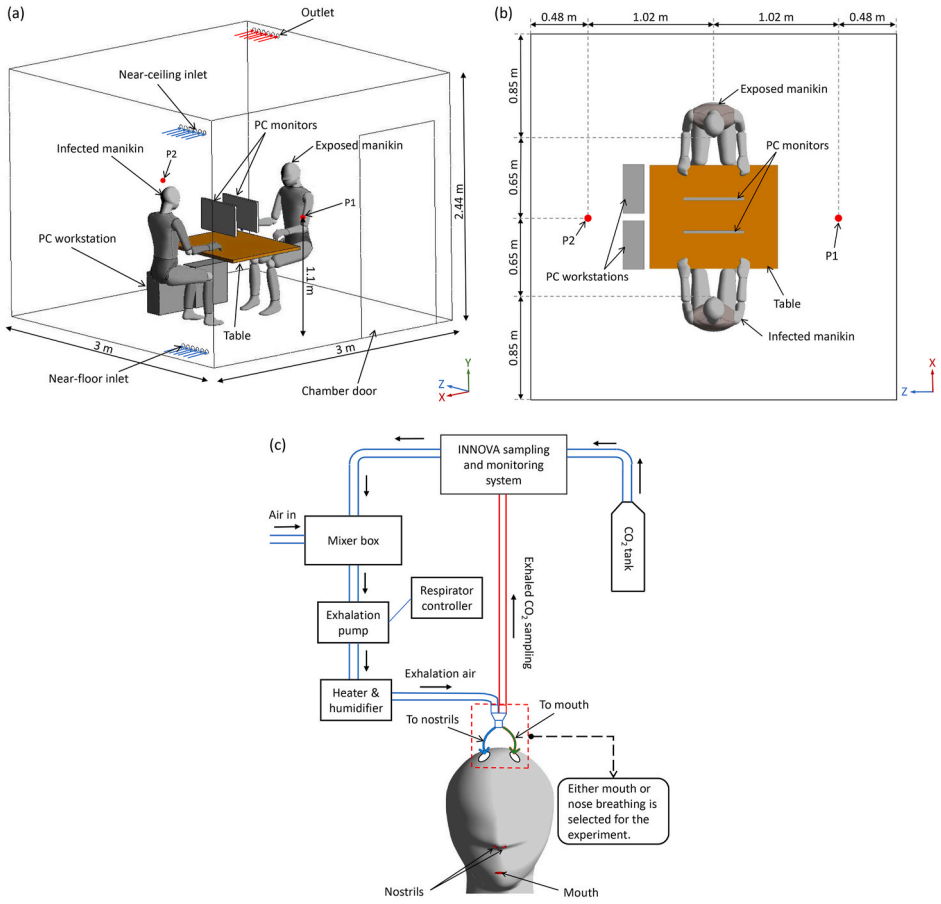


**Fig. 2.** A schematic sketch of (a) experimental configuration in the climate chamber; (b) top view of the measurement setup; (c) breathing system of the infected manikin.

positioned at a height of 1.1 m from the floor, with a distance of about 45 cm from the adjacent walls. The INNOVA monitor (operating based on the photoacoustic principle) achieved a sampling rate of 3.3 min per data set and has an expanded uncertainty equal to 3 % of the reading. It should be noted that the sampling rate of the INNOVA monitor is related to the number of activated channels, which were six during the experiments (from which only five channels were used for the data analysis)

The experiments were executed under virtually steady-state conditions, wherein the room air temperature was stabilized within ±0.1 K. Additionally, the concentration-time curve at the ventilation exhaust demonstrated a slope of less than 10 mg/m$^3$ (5.5 ppm) per 10 min. To attain a time-independent mean value during the experiments, it was imperative to amass a sufficient volume of samples. In Ref. [43], the recommended minimum required sample quantity from the INNOVA system for assessing exposure risk is 15 samples. Hence, in this study, 20 samples from the INNOVA were collected for each experiment. As the sampling interval for the ALMEMO $CO_2$ sensor was 1 s, while it was 3.3 min for INNOVA (with five sampling channels activated corresponding to five sampling locations), the time required by the INNOVA to accumulate the targeted 20 samples offered a substantial window for the ALMEMO $CO_2$ sensor to establish a time-independent mean value with approximately 2000–3000 samples. In each experiment, a quasi steady-state was achieved approximately 105 min after the infected manikin commenced $CO_2$ dosing. To calculate exposure and assess the risk of infection, it took about 67 min to collect 20 samples using the INNOVA system. The experimental time schedule is shown in Fig. 3.

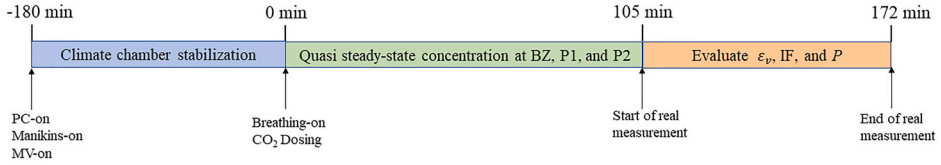


**Fig. 3.** The time schedule of the experiments.

### 2.3. Experimental conditions

As Liu et al. [48] demonstrated superior performance of wall-supplied MV over ceiling-supplied MV regarding CRE, for this study, wall-mounted MV supply was also used. The experiments were performed using two different MV configurations: near-ceiling and near-floor inlet, both with near-ceiling exhaust (Fig. 2, a). In addition to altering the configuration of the MV system, three additional parameters were varied: (a) ACH, (b) breathing pattern, and (c) supply temperature. The formulation of these experimental conditions was predicated on achieving a balance between available experimental resources and the primary objective of evaluating the characteristics of airborne transmission within different configurations of the indoor environment. Four ACH were investigated in this study: 1.2, 2, 4, and 6.6 $h^{-1}$, which were chosen to align with the ventilation categories defined in EN 16798–1 [49] (Table 1). As for the breathing pattern, both nose breathing and mouth breathing were studied as they both correspond to the quiescent breathing associated with seated occupants engaged in typical office tasks. Additionally, two supply air temperatures, namely 19 °C and 21 °C, were considered to evaluate the impact of supply temperature on IAQ. The average temperature of all body segments of the exposed manikin was 33 °C and 33.4 °C under a supply temperature of 19 °C and 21 °C, respectively. A total of 24 different scenarios were investigated in this study. A comprehensive overview of the experimental scenarios and conditions is shown in Table 2.

### 2.4. Evaluation indexes

#### 2.4.1. Ventilation effectiveness ($\varepsilon_v$)

The ventilation effectiveness ($\varepsilon_v$) is a critical metric used in assessing the efficiency of ventilation systems within enclosed spaces. The $\varepsilon_v$ serves as a quantitative measure to evaluate the dispersion and dilution of contaminants within a given environment. The steady index of the $\varepsilon_v$ was first proposed by Sandbere [50] to express how the system's ventilation ability varies between different parts of a room. For MV, the $\varepsilon_v$ values typically range from 0 to 1, with higher values indicating more effective ventilation in reducing contaminant concentration levels within occupied spaces. The $\varepsilon_v$ is widely utilized in building design, HVAC engineering, and indoor air quality research to evaluate the performance of ventilation strategies and optimize their efficacy [51,52]. The $\varepsilon_v$ is calculated as follows:

$$\varepsilon_v = \frac{\overline{C_e} - \overline{C_s}}{\overline{C_a} - \overline{C_s}} \tag{1}$$

Where $\overline{C_e}$, $\overline{C_s}$, and $\overline{C_a}$ are the average concentration at the exhaust, supply, and any point inside the climate chamber. In this study, the ventilation effectiveness was monitored at P1 and P2 to evaluate IAQ in the room.

While $\varepsilon_v$ serves as a valuable metric for evaluating ventilation system efficacy, it does not inherently determine the system's effectiveness in mitigating exposure to airborne contaminants. For instance, a study by Chen and Zhao [53] demonstrated that while $\varepsilon_v$ can improve air distribution, it does not guarantee effective removal of viral contaminants or reduction in infection risk. Additionally, research by Rudnick and Milton [54] emphasized the complex interplay between ventilation rate, airflow patterns, and other factors such as occupancy and airborne contaminates distribution, which can influence the effectiveness of ventilation systems in reducing airborne pathogen transmission. Therefore, the literature recommends complementing $\varepsilon_v$ with other air quality metrics to comprehensively evaluate the ability of ventilation systems to mitigate infection risk and remove airborne contaminants [53,54]. Therefore, this study also employs the evaluation of exposure risk and infection risk to comprehensively evaluate the influence of ACH, MV modes, breathing pattern, and supply temperature on mitigating the risk of airborne contaminants.

#### 2.4.2. Exposure risk

The assessment of exposure to exhaled contaminants within the BZ of the exposed manikin was conducted through the utilization of intake fraction (*IF*). The *IF* is defined as the ratio of the contaminants inhaled by an exposed occupant to the contaminants exhaled by the infected occupant [55]. The greater the *IF*, the greater the exposure risk [5]. *IF* can be calculated as follows:

$$IF = \frac{\overline{C_{exp}}}{\overline{C_{inf}}} \tag{2}$$

where $\overline{C_{exp}}$ and $\overline{C_{inf}}$ are average concentrations measured at the BZ of the exposed manikin and exhalation of the infected manikin subsequent to achieving a stabilized concentration. However, considering the presence of $CO_2$ in the ventilation supply air, the calculation of the *IF* in Equation (2) necessitates the use of a background-corrected ratio, as follows:

**Table 1**
The investigated ACH and their corresponding EN 16798–1 ventilation categories [49]. The ACH ranges reported in parentheses are determined based on the number of occupants and the area of the climate chamber.

| Climate chamber ACH [$h^{-1}$] | Corresponding EN 16798–1 ventilation category |
|---|---|
| 1.2 | Category IV (1.1–1.7 $h^{-1}$) |
| 2 | Category III (1.6–2.5 $h^{-1}$) |
| 4 | Category II (2.8–4.4 $h^{-1}$) |
| 6.6 | Category I (4–6.2 $h^{-1}$) |

**Table 2**
The experimental scenarios investigated in this study.

| Scenarios | MV configuration | Breathing pattern | Supply Temperature [°C] | ACH [$h^{-1}$] |
|---|---|---|---|---|
| 1–4 | Near-ceiling inlet | Nose | 21 | 1.2, 2, 4, and 6.6 |
| 5–8 | Near-ceiling inlet | Mouth | 21 | 1.2, 2, 4, and 6.6 |
| 9–12 | Near-floor inlet | Nose | 21 | 1.2, 2, 4, and 6.6 |
| 13–16 | Near-floor inlet | Mouth | 21 | 1.2, 2, 4, and 6.6 |
| 17–18 | Near-ceiling inlet | Nose | 19 | 2 and 4 |
| 19–20 | Near-ceiling inlet | Mouth | 19 | 2 and 4 |
| 21–22 | Near-floor inlet | Nose | 19 | 2 and 4 |
| 23–24 | Near-floor inlet | Mouth | 19 | 2 and 4 |

$$IF = \frac{\overline{C_{exp-}C_{bkg}}}{\overline{C_{inf}}} \tag{3}$$

where $\overline{C_{bkg}}$ represents the average background $CO_2$ concentration at the BZ of the exposed manikin prior to initiating $CO_2$ dosing through the infected manikin. The determination of the $C_{bkg}$ value was conducted subsequent to achieving a stabilized concentration, maintained for an average duration of 5 min, preceding the start of the infected manikin's breathing. The employed methodology, consistent with numerous prior studies [56,57], entails measuring the naturally occurring background $CO_2$ levels at each measuring point within the chamber before the initiation of the manikin's breathing. Subsequently, these initial background levels were subtracted from the total $CO_2$ concentration at each measurement point post-dosing, once a state of stabilization was achieved. It is essential to highlight that $C_{inf}$ was measured within the breathing tubing of the infected manikin (Fig. 1, left) and not within the room itself. Consequently, the background concentration in the room was not subtracted from $C_{inf}$ when calculating *IF*.

### 2.4.3. Infection risk

Riley et al. [58,59] introduced the Wells-Riley equation in 1978 as a framework for investigating the airborne transmission of measles. Unlike exposure risk, this approach requires the quanta emission rate of a specific virus. Therefore, this study evaluated the relationship between ventilation and probability of airborne infection of SARS-CoV-2 as an example virus that is often used in recent studies. The probability of infection can be calculated using the following equation:

$$P = 1 - e^{-\frac{I \bullet q \bullet p \bullet t}{Q}} \tag{4}$$

where $P$ is the probability of infection; $I$ number of infected occupants; $q$ quanta emission rate by the infected occupants (quanta/h); $p$ breathing rate of healthy occupants ($m^3$/h); $t$ is the exposure time interval (h); and $Q$ is the space ventilation rate ($m^3$/h).

According to Equation (4), the Wells-Riley model exclusively evaluates the collective probability of infection, assuming a homogeneous distribution throughout the confined space. Consequently, its application is restricted to situations characterized by perfect spatial homogenization, rendering it inadequate to estimate infection risk in scenarios with non-mixed conditions [5,60]. However, real-world environmental contexts exhibit non-uniform air dispersion dynamics, leading to disparate distribution patterns of infectious pathogens. Hence, the spatial accuracy constraints inherent in the Wells-Riley model when estimating infection risk may lead to either overestimation or underestimation of airborne infection risk. Considerable efforts have been dedicated to utilizing the Wells-Riley model for evaluating infection susceptibility in environments characterized by non-uniform conditions [61–63]. In this investigation, the dilution-based assessment technique introduced by Zhang and Lin [64] was employed to obtain the quanta distribution in the climate chamber. The dilution ratio ($D$) was used to calculate the inhaled quanta at the BZ of the exposed manikin using the following equation:

$$D = \frac{\overline{C_{inf}}}{\overline{C_{exp}} - \overline{C_{bkg}}} \tag{5}$$

Consequently, the Wells-Riley model can be adapted to:

$$P = 1 - \exp\left(-\frac{I \bullet q \bullet t}{D}\right) \tag{6}$$

The value of t is taken as 1 h' which is the most common used value to evaluate the infection risk in the literature [62,65]. As for q, the previous studies involving the assessment of the infection risk of SARS-CoV-2 utilized different q values for calm breathing. A study by Liu et al. [66] employed a q value of 36.6 quanta/h for evaluating the infection risk in multi-room building. Su et al. [67] and Qin et al. [68] utilized a lower value of 10.5 quanta/h for assessing the risk of SARS-CoV-2 in a densely occupied spaces. According to Dai and Zhao [69], q spans from 14 to 48 quanta/h under calm breathing. This upper limit (48 quanta/h) was used by several studies in the literature such as Dai et al. [70], Fageha and Alaidroos [71], Hatif et al. [72], Park et al. [73], and Zhang et al. [62]. Hence, in alignment with these studies, this study also uses a q value of 48 quanta/h to evaluate the infection risk of SARS-CoV-2.

## 3. Results and analysis

### 3.1. Ventilation effectiveness ($\varepsilon_v$)

Fig. 4 illustrates the impact of ACH, MV configuration, breathing pattern and the supply temperature on $\varepsilon_v$ at P1. The analysis shows a clear trend: as ACH increases, $\varepsilon_v$ decreases, indicating a negative correlation. Specifically, at an ACH of 1.2 $h^{-1}$, $\varepsilon_v$ ranged from 0.69 to 0.79. Increasing ACH to 2 $h^{-1}$ reduced $\varepsilon_v$ to a range between 0.57 and 0.69. A further increase to 6.6 $h^{-1}$, a 5.5-fold increase, significantly lowered $\varepsilon_v$ to a range between 0.22 and 0.34. The study also examined how MV configuration affects $\varepsilon_v$. At lower ACH rates, a near-ceiling inlet generally produced slightly higher $\varepsilon_v$ values, with a difference ranging from 0.05 to 0.1 compared to a near-floor inlet. However, at higher ACH levels (4 and 6.6 $h^{-1}$), the near-floor inlet configuration was more effective, surpassing near-ceiling configurations by approximately 0.05–0.11. Regarding the influence of breathing patterns and supply temperature on $\varepsilon_v$, the results indicated that breathing patterns did not significantly influence $\varepsilon_v$ values. Similarly, variations in supply temperature showed no substantial impact on $\varepsilon_v$ at ACH of 2 $h^{-1}$. However, at an ACH of 4 $h^{-1}$, reducing the supply temperature from 21 °C to 19 °C led to a slight increase in $\varepsilon_v$ values, ranging from 0.02 to 0.06.

Fig. 5 shows the values of $\varepsilon_v$ across all investigated scenarios at P2. The results indicated that the values of $\varepsilon_v$ generally increased with larger ACH in most cases. However, the scenario involving a near-floor inlet and nose-breathing with a supply temperature of 21 °C exhibited significant variability. This may be attributed to various parameters which are explained in the last paragraph of this subsection.

The results showed that increasing the ACH from 2 $h^{-1}$ to 6.6 $h^{-1}$ caused $\varepsilon_v$ values to increase from a range of 0.86–1.04 to 1.16–1.39, respectively. Notably, $\varepsilon_v$ values at position P2, which ranged from 0.79 to 1.39, exceeded those at P1 (0.69–0.79) by 0.1–0.6. The significance of these findings will be discussed in the following paragraph. Additionally, $\varepsilon_v$ values at P2 often surpassed the typical values around 1 for conventional MV systems [6], even at lower ACH levels. Regarding the impact of different MV modes, the near-ceiling inlet generally performed better than the near-floor inlet across all ACH rates, except under two specific conditions: at an ACH of 1.2 $h^{-1}$ with nose breathing, where the difference was marginal (about 0.03), and at an ACH of 6.6 $h^{-1}$ with nose breathing, where the near-floor inlet outperformed the near-ceiling by 0.23 ($\varepsilon_v$ of 1.39 compared to 1.16). This variance is likely attributable to random errors, which are often induced by uncontrollable factors, such as environmental conditions, as discussed in detail in the final paragraph of this subsection. Similar to findings at P1, neither breathing patterns nor supply temperature significantly affected the $\varepsilon_v$ values at P2.

The variation in $\varepsilon_v$ between positions P1 and P2 can be attributed to several fluid dynamics' factors. Firstly, the placement of supply inlets and exhaust outlets is crucial. In the case of a near-ceiling inlet, the supply is positioned at a height of 2.4 m, while for a near-floor inlet, it is at 0.2 m. Both are closer to P1 (as shown in Fig. 2a). The exhaust outlet for both modes is positioned at 2.4 m and is closer to P2. This configuration, in which the supply inlets are on one side of the room and the exhaust outlet is on the other side of the room, creates a directional airflow pattern which results in a more efficient distribution of fresh air towards the far side of the room where P2 is located. This resulted in increased values of $\varepsilon_v$ at P2 compared to P1. Secondly, P1 is situated at a height of 1.1 m, which is either below or above the path of clean supply air jets from the near-floor and near-ceiling inlets, respectively. This positioning results in reduced ventilation effectiveness at P1 as the clean supply air mixes with the room's contaminated air before reaching this point.

### 3.2. Intake fraction (IF)

Fig. 6 presents the average *IF* values for the exposed manikin across various scenarios. The analysis indicates a significant reduction in *IF* values with increased ACH. Specifically, increasing the ACH to 2 $h^{-1}$ reduced the *IF* by 24.4 %–62 % across all scenarios compared

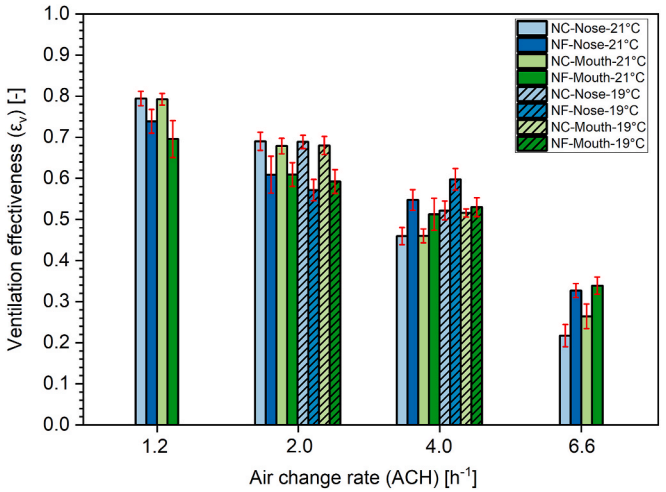


**Fig. 4.** The average ventilation effectiveness ($\varepsilon_v$) at P1. NC refers to near-ceiling inlet while NF refers to near-floor inlet; the error bars represent the standard deviation of the measurements.

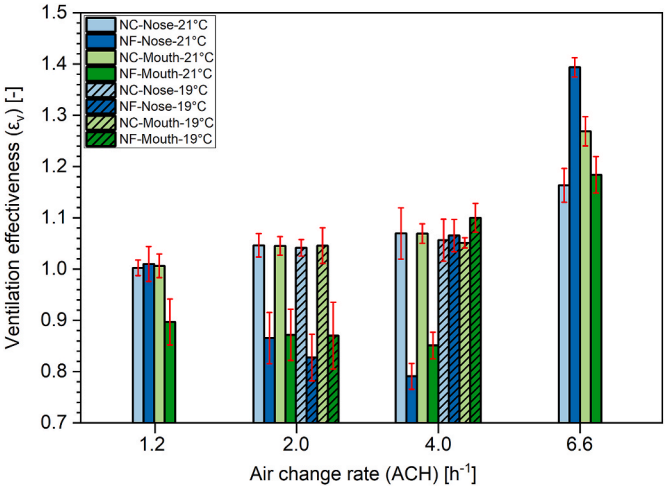


**Fig. 5.** The average ventilation effectiveness ($\varepsilon_v$) at P2. NC refers to near-ceiling inlet while NF refers to near-floor inlet; the error bars represent the standard deviation of the measurements.

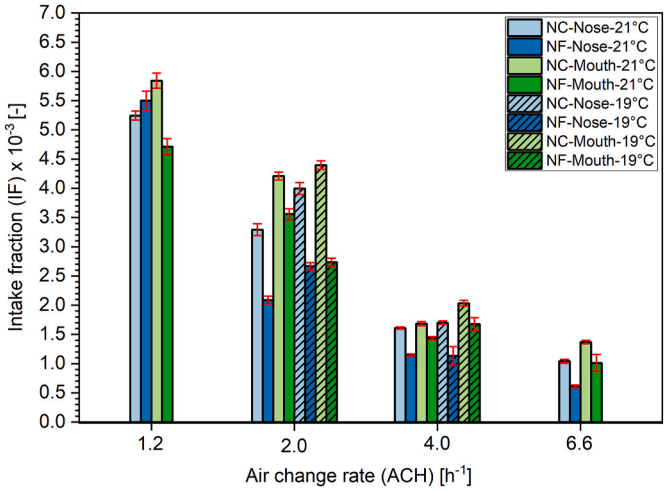


**Fig. 6.** The average intake fraction (*IF*) at the breathing zone of the exposed manikin under all investigated scenarios. NC refers to near-ceiling inlet while NF refers to near-floor inlet; the error bars represent the standard deviation of the measurements.

to an ACH of 1.2 $h^{-1}$. For example, under conditions of a near-ceiling inlet, nose breathing, and a supply temperature of 21 °C, increasing the ACH to 2 $h^{-1}$ decreased the *IF* by 37.2 % (from $5.02 \times 10^{-3}$ to $3.29 \times 10^{-3}$). Further increasing ACH to 4 $h^{-1}$ resulted in an additional reduction of *IF* values by 69.3 %–79.9 % relative to an ACH of 1.2 $h^{-1}$. For instance, for the conditions described above (near-ceiling inlet, nose breathing, and supply temperature of 21 °C), raising the ACH to 4 $h^{-1}$ led to a tripling of the *IF* reduction (from $5.02 \times 10^{-3}$ to $1.6 \times 10^{-3}$). The highest ventilation rate tested, 6.6 $h^{-1}$, decreased the *IF* by 75.5 %–80.2 % in all investigated cases. For instance, under the aforementioned conditions, an ACH of 6.6 $h^{-1}$ reduced the *IF* by nine-fold (from $5.49 \times 10^{-3}$ to $0.61 \times 10^{-3}$) compared to an ACH of 1.2 $h^{-1}$.

The changes in *IF* when increasing ACH can be attributed to three significant effects of higher ACH on the distribution of exhaled airborne contaminants. The first effect is increasing dispersion, attributed to the heightened indoor air movement. The second effect is the enhanced dilution due to the increased indoor air replacement. The third effect is altering the flow interaction within the BZ due to the expanded spread of the supply flow. These three effects collectively influence the mean *IF* index at various ACH values, thereby determining the risk of cross-exposure risk.

The location of the supply air diffuser can have an influence on the cross-exposure risk. The result showed that transitioning from near-ceiling inlet to near-floor inlet under ACH of 1.2 $h^{-1}$ (with nose breathing and supply temperature of 21 °C) slightly increased the *IF* from $5.24 \times 10^{-3}$ to $5.49 \times 10^{-3}$. Yet, under all other investigated scenarios, the near-floor inlet showed improved *IF* values. The results also highlighted that the higher ACH, the more efficient near-floor inlet is compared to near-ceiling inlet in mitigating the exposure risk to airborne contaminants. Specifically, adapting near-floor inlet at an ACH of 6.6 $h^{-1}$ reduced the *IF* values by 1.7 times ($1.04 \times 10^{-3}$ to $0.61 \times 10^{-3}$) under nose breathing.

The effect of the MV configurations reported in this study on the spread of the exhaled contamination can have different reasons. Firstly, there was an improvement in contaminants removal efficiency, as the supply flow jet in the case of the near-floor inlet was positioned below the level of the head and the BZ of the infected manikin. This facilitated the movement of clean air from the lower region of the room to the upper region, contrasting with the air movement from the room's upper region to the room's upper region in the case of a near-ceiling inlet. Secondly, altering the flow interaction within the BZ of the infected manikin occurred due to air movement from the lower region of the room. These combined effects influenced the mean *IF* index at different ACH values, thereby determining the risk of cross-exposure risk.

In addition to ACH and MV configuration, the choice between mouth and nose breathing significantly affected the spread of airborne contaminants, and consequently, the *IF* at the BZ of the exposed manikin. As shown in Fig. 6, under low ACH (1.2 $h^{-1}$), the MV ventilation pattern significantly influences which breathing pattern poses the highest exposure to airborne contaminants. At a low ACH of 1.2 $h^{-1}$, the type of breathing pattern markedly affects exposure levels. For instance, under a near-ceiling inlet, mouth breathing resulted in an *IF* that was 11.5 % higher than nose breathing. Conversely, under a near-floor inlet, mouth breathing led to a 14.4 % lower *IF* compared to nose breathing, demonstrating that at lower ACH levels (1.2 $h^{-1}$), the *IF* associated with mouth breathing is not consistently higher than that with nose breathing. As ACH increases to 2 $h^{-1}$, the disparity between the breathing patterns becomes more pronounced, with mouth breathing leading to *IF* values 28 %–70.3 % higher than those associated with nose breathing across all scenarios. For example, adopting the highest recommended ventilation rate (ACH of 6.6 $h^{-1}$) showed that mouth breathing had significantly higher *IF* values than nose breathing with an increase range of 31.7 %–65.2 % across all investigated scenarios. Thus, our study showed that the difference in *IF* across breathing modes is more significant at higher ventilation rates.

When inspecting Fig. 6, it is clear that mouth breathing generally leads to a greater dispersion of contaminants compared to nose breathing. This distinction is attributed to the airflow dynamics and release of contaminants associated with each breathing pattern. For example, nose breathing typically involves a slower and more controlled airflow, which tends to result in reduced dispersion of contaminants compared to the faster and more turbulent airflow associated with mouth breathing. These differing breathing patterns collectively influence the mean *IF* across various MV configurations and ACH, thereby influencing the risk of cross-infection. Therefore, considering the effects of breathing patterns on contaminant spread is essential for correct evaluation of airborne transmission in indoor environments. However, it is essential to acknowledge that in real-world scenarios, the control over whether an individual breathes through the nose or mouth is unattainable. Nonetheless, when conducting studies aimed at optimizing the indoor environment, the choice of the implemented breathing pattern is imperative. Understanding which breathing pattern contributes to a higher infection risk allows for the selection of worst-case scenarios, thereby enabling a comprehensive assessment of the efficacy of various ventilation systems and other environmental scenarios. This underscores the significance of carefully considering the type of breathing pattern in empirical studies as well as in numerical simulations for accurate and informed analyses of infection transmission dynamics.

Fig. 6 also demonstrates the significant role of supply air temperature in ventilation systems on the spread of exhaled air and the potential for cross-infection. The impact varies significantly with the MV configuration and ACH. At an ACH of 2 $h^{-1}$, the MV configuration crucially influences the relationship between supply temperature and *IF* for the same breathing pattern. For instance, under conditions of a near-ceiling inlet, the *IF* at a supply temperature of 19 °C was 4.3 %–17.7 % higher than at 21 °C for both nose and mouth breathing scenarios. In contrast, under near-floor inlet conditions, a supply temperature of 19 °C resulted in a 21.7 % decrease in IF for mouth breathing but a 29.9 % increase for nose breathing.

Increasing ACH from 2 $h^{-1}$ to 4 $h^{-1}$ showed no significant difference in *IF* between the supply temperatures of 21 °C and 19 °C for both MV configurations under nose breathing patterns. However, a slight increase in *IF* was observed under mouth breathing at 19 °C. These findings indicate that a lower supply temperature does not consistently correlate with higher cross-infection risks. The influence

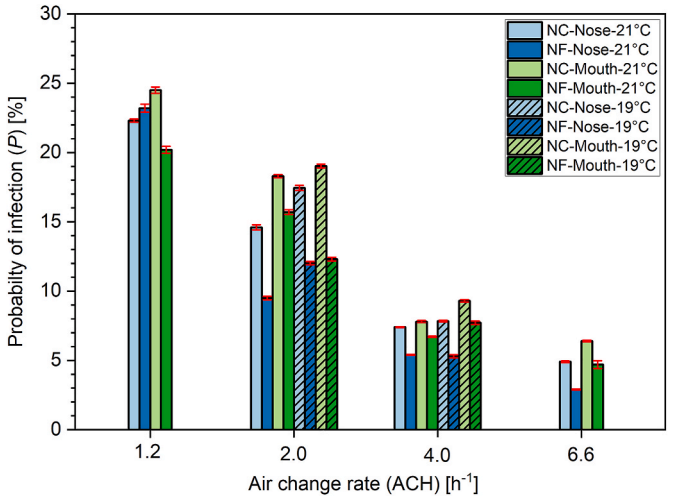


**Fig. 7.** The average values of infection probability (*P*) calculated for the exposed manikin under all investigated scenarios. NC refers to near-ceiling inlet while NF refers to near-floor inlet; the error bars represent the standard deviation of the measurements.

of supply temperature on *IF* is complex, mediated by factors such as changes in the convective boundary layer intensity and the thermal plume around the human body, along with alterations in the direction of breathing flows. For example, the average indoor air temperature at 1.1 m and near-ceiling inlet with an ACH of 4 $h^{-1}$ was 25.6 °C (±0.05) and 26.5 °C (±0.06) under the supply temperature of 19 °C and 21 °C, respectively. Additionally, the average temperature of all body segments of the exposed manikin was 33 °C and 33.4 °C under a supply temperature of 19 °C and 21 °C, respectively. A smaller temperature differential between the indoor air temperature and the surface of the thermal manikin tends to result in a thicker boundary layer because the driving force for convective heat transfer (the temperature gradient) is reduced. Additionally, a thicker boundary layer can act somewhat like a 'protective' layer around the human body, potentially slowing down the movement of contaminants towards the body. This is because the boundary layer serves as a region of slowed airflow near the surface, where the velocity gradient changes from zero at the surface (no-slip condition) to the free-stream velocity further away from the surface. Therefore, the increase in indoor air temperature to 26.5 °C with a manikin surface temperature of 33.4 °C (compared to the previous condition of 25.6 °C indoor and 33 °C surface temperature) suggests an increased thickness of the boundary layer which as a result reduced the exposure risk. Finally, the results showed that under most cases lower supply air temperatures tend to result in a slight increased dispersion of contaminants, potentially leading to elevated contaminant levels between occupants. This disparity in contaminant distribution is influenced by the airflow and contaminant release dynamics associated with each breathing pattern, underscoring the importance of considering supply air temperature and breathing patterns when assessing cross-exposure risks.

### 3.3. Infection probability (P)

The implemented infection probability index (*P*) in this study measures the probability of infection on a scale from 0 to 1, where 1 represents a 100 % infection risk. For clearer understanding, *P* values are expressed as percentages. Fig. 7 shows the average values of *P* across all investigated cases. The findings showed that increasing the ACH resulted in trends similar to those observed in *IF* values. For example, at an ACH of 1.2 $h^{-1}$, *P* values ranged from 20.2% to 24.5 % across all cases. Increasing the ACH to 2 $h^{-1}$ led to a decrease in *P* values to between 9.5 % and 18.3 %, reflecting a reduction of 22.3 %–34.5 % from the lower ACH (1.2 $h^{-1}$). At the highest tested ACH of 6.6 $h^{-1}$, *P* values further dropped to between 2.9 % and 6.4 %, depending on the specific ventilation mode and breathing pattern analyzed. This data highlights the effectiveness of increased ventilation rates in significantly lowering the probability of infection.

The analysis also highlights the significant role of MV configurations in mitigating infection risk. The near-floor inlet configuration consistently proves to be more effective than the near-ceiling counterpart across various ACH. For example, at an ACH of 2 $h^{-1}$, switching to a near-floor inlet from a near-ceiling inlet resulted in a reduction of *P* values from 14.6%-18.3 % to 9.5%–15.7 %. The efficiency of the near-floor inlet increased with higher ACH levels. At an ACH of 6.6 $h^{-1}$, using a near-floor inlet under the nose breathing scenario led to a decrease in *P* values from 4.9 % to 2.9 %. This trend underscores the enhanced capability of near-floor inlets to mitigate infection risk from airborne contaminants as ventilation rates increase.

The analysis also highlights the significant role of breathing patterns in determining infection risk. It reveals that mouth breathing generally leads to higher *P* than nose breathing, especially at higher ACH (2, 4, and 6.6 $h^{-1}$). For instance, at an ACH of 2 $h^{-1}$ with a near-floor inlet, mouth breathing increased the *P* value from 15.7 % to 18.3 % compared to nose breathing. This trend intensified with an increase in ACH to 6.6 $h^{-1}$, showing a larger difference in *P* values between mouth and nose breathing. However, an exception was noted at a lower ACH of 1.2 $h^{-1}$ with a near-floor inlet, where mouth breathing resulted in a lower *P* value than nose breathing, as illustrated in Fig. 7. This indicates that mouth breathing does not consistently pose a higher risk of cross-infection compared to nose breathing, particularly under certain ventilation configurations. This finding highlights the complex interplay between breathing patterns and ventilation systems in modulating infection risk.

Regarding the influence of supply temperature on the values of infection risk, our study showed that lower supply temperatures resulted in higher infection risk compared to higher supply temperatures, especially at lower ACH (2 $h^{-1}$). For instance, under an ACH of 2 $h^{-1}$ and a near-ceiling inlet with nose breathing, the *P* value at a supply temperature of 19 °C was 19.2 % higher than at 21 °C, increasing from 14.6 % to 17.4 %. However, when the ACH was increased to 4 $h^{-1}$, there was no significant difference in *P* values between the two temperatures for both MV configurations and nose breathing patterns. A notable difference was observed under the near-ceiling MV configuration with mouth breathing, indicating that infection risk varies significantly with different breathing patterns. Therefore, the correlation between lower supply temperatures and increased infection risk is not uniform across all conditions. Instead, the MV configuration and breathing patterns significantly influence how different supply temperatures impact the risk of cross-infection.

## 4. Discussion

The results of our study showed that $\varepsilon_v$ values varied significantly between different measuring points due to factors such as the positioning of the supply inlet and exhaust outlet, as well as the location of the measuring point. For instance, at P1, increasing the ACH from 1.2 to 6.6 $h^{-1}$ led to a decrease in $\varepsilon_v$ from 0.75 to 0.55, while at P2, the same increase in ACH resulted in an improvement in $\varepsilon_v$ from 0.60 to 0.85. These findings highlight the non-uniform impact of ACH on $\varepsilon_v$, influenced by specific airflow dynamics at different points within the space. This variability suggests that the $\varepsilon_v$ index alone may not be sufficient for evaluating the efficiency of ventilation systems in mitigating exposure and infection risk from airborne contaminants. Metrics such as *IF* and *P* should be used alongside $\varepsilon_v$ for a more comprehensive assessment of ventilation performance. These results are similar to previous studies conducted by Chen and Zhao [53] were they demonstrated that while a higher $\varepsilon_v$ can improve air distribution, it does not guarantee an effective removal of viral contaminants or a reduction in infection risk.

Our findings also revealed a consistent correlation between increasing ACH and reductions in both *IF* and *P*. For example,

transitioning from an ACH of 1.2 $h^{-1}$–6.6 $h^{-1}$ reduced *IF* from 0.045 to 0.015 and *P* from 11 % to 3.5 % under near-floor inlet conditions with nose breathing. These results differ from previous studies that suggested higher ACH could increase cross-exposure risk. A key distinction in our study is the replication of a realistic office environment, including equipment such as PC monitors and workstations as well as complex thermal breathing manikins, which may not have been fully represented in earlier research. This more accurate setup likely contributed to the differing outcomes observed in our study [8,11,13]. Another reason is that the discrepancy may be attributed to the complexity of flow interactions within the BZ, particularly at closer distances (less than 1.2 m), where linear dependence on ACH changes may not apply [8,74]. The results also showed that even at the maximum ACH (6.6 $h^{-1}$, Category I), the minimum *P* value achieved was approximately 2.9 %, indicating that even the highest ventilation category recommended by EN 16798-1 might not be sufficient to achieve an infection risk lower than 1 %, as suggested by Dai and Zhao [69]. Therefore, conventional MV systems should be combined with add-on devices such as personalized ventilation, portable air cleaners, and Upper-Room Ultraviolet Germicidal Irradiation to further mitigate infection risk in indoor environments [47]. Additionally, adopting a moderate ventilation category (e.g. Category III) in conjunction with add-on systems (e.g. air cleaners) might be a good approach to reduce energy consumption compared to adopting MV alone with a better ventilation category (e.g. Category I).

Regarding the influence of the MV ventilation configuration, the study showed that the near-floor inlet configuration consistently outperformed the near-ceiling inlet in reducing *IF* and *P* across all ventilation categories outlined in the EN 16798-1 standard. Specifically, *IF* values were 15–41 % lower, and *P* values were reduced by up to 65 % in the near-floor configuration compared to the near-ceiling configuration. Specifically, switching to a near-floor inlet generally enhanced contaminant removal across all adapted EN 16798–1 ventilation categories for mouth breathing and across three categories (III, II, and I) for nose breathing. These results were especially pronounced under high ACH scenarios, where the near-floor inlet was particularly effective in reducing contamination in the BZ. These findings are consistent with previous studies that have demonstrated the efficacy of MV systems with near-floor supply and near-ceiling exhaust configurations in reducing contaminant concentrations compared to setups with low-exhaust and high-supply or high-exhaust and high-supply designs [13,19,20]. This underscores the critical role of ventilation design and configuration in mitigating airborne infection transmission, providing valuable insights for optimizing IAQ and enhancing occupant safety in various settings. Such findings emphasize the importance of ventilation design and configuration in mitigating airborne transmission risks.

The breathing pattern also showed a notable impact on the values of *IF* and *P*. Our results challenge the conventional assumption that mouth breathing consistently poses a higher risk of cross-infection compared to nose breathing across various ventilation configurations. Specifically, in the context of EN 16798-1 Category IV ventilation (ACH of 1.2 $h^{-1}$), we observed that only one configuration resulted in lower *IF* for mouth breathing compared to nose breathing. This occurred with a ventilation setup featuring a near-ceiling inlet at an ACH of 1.2 $h^{-1}$, highlighting how ventilation design can significantly influence contaminant dispersion among occupants. Moreover, as ventilation rates increased to those specified by EN 16798-1 Category I (ACH of 6.6 $h^{-1}$), the differences in infection risk between mouth and nose breathing became more pronounced. For example, under near-floor inlet conditions with an ACH of 6.6 $h^{-1}$, mouth breathing led to a 31.7 %–65.3 % higher *IF* than nose breathing. These findings underscore that the infection risk for an exposed occupant is generally greater with mouth breathing, particularly at higher ventilation rates.

The analysis also indicated that lower supply temperatures consistently increased *IF* and *P*, particularly under near-ceiling inlet configurations. For example, reducing the supply temperature from 21 °C to 19 °C increased *IF* by 12–18 % and *P* by 10–15 %. The higher infection risk associated with lower supply air temperatures in a room occupied by two occupants can be attributed to several factors. Firstly, in a near-ceiling inlet scenario, the contaminants concentration at the floor level is higher compared to a near-floor scenario. Secondly, with stronger convection around the body, more contaminants are transported into the breathing zone from the lower part of the room. The findings suggest that while lower temperatures can exacerbate infection risks, the specific ventilation configuration and breathing patterns play a more critical role in determining these outcomes.

In conclusion, the findings of this study underscore the importance of considering multiple factors when designing ventilation strategies to mitigate airborne transmission in indoor environments. However, it is important to point out that the reported results were acquired using tracer gas as a surrogate for exhaled droplet nuclei. The dispersion behavior of larger particles may vary under horizontal air supply flow conditions compared to tracer gas. Further, it must be noted that quiescent breathing implemented in this study may not be a primary transmission source in office settings, where emissions from speaking, coughing, and sneezing, which produce larger droplets, could dominate. Given the distinct ejected particle sizes and exhaled airflow patterns associated with these activities compared to quiescent breathing, addressing this limitation necessitates further investigations and analysis. Finally, while the findings of this study highlight the dispersion of exhaled air from the infected manikin into the indoor environment, the precise time it takes to reach different room areas remains unknown as the study was conducted under steady-state. Understanding this dissemination timeframe in relation to the typical survival duration of pathogens can be crucial for accurately assessing the risk of cross-infection. Further research is warranted to address these limitations and refine ventilation guidelines for enhanced occupant safety.

## 5. Conclusion

This study explored the dynamics of airborne transmission in an office environment, focusing on the influence of several factors on IAQ, namely ACH, MV ventilation configuration, breathing pattern, and supply air temperature. The findings highlight several critical insights with broader implications for improving the indoor environment and mitigating airborne infection risks.

Firstly, the results demonstrate that $\varepsilon_v$ is highly sensitive to the spatial probing point and airflow patterns. This highlights the complexity of airflow in indoor environments, where the placement of ventilation inlets and outlets, along with occupant positions, can significantly affect air distribution and contaminant removal. This complexity suggests that relying solely on traditional metrics

like $\varepsilon_v$ may not be sufficient for evaluating ventilation performance. A combination of metrics, such as *IF* and *P*, is recommended for future studies on this topic for a more comprehensive assessment of the risk of airborne transmission, particularly in environments with varied airflow patterns. Secondly, the study underscores the consistent reduction of infection risk with increasing ACH, which improves contaminant dilution and removal. However, this effect is not uniform across all conditions, emphasizing the importance of ventilation design. For example, near-floor inlet configurations were more effective in displacing contaminated air from the BZ compared to near-ceiling inlets. These findings reinforce established fluid dynamics principles and provide practical guidance for ventilation system design, particularly in settings where IAQ is a priority.

Moreover, this study contributes new insights into how occupant behavior, specifically breathing patterns, affects infection risk. This study illustrated that mouth breathing was generally associated with higher infection risk compared to nose breathing, especially at higher ACH levels. These findings are highly relevant for other researchers conducting manikin measurements or CFD simulations, in which the experimental and numerical configurations have a major influence on the acquired results.

This study also showed that the overall influence of ventilation configuration and occupant behaviour plays a more significant role compared to the supply air temperature, even though lower supply temperatures were found to increase infection risk under certain conditions. This emphasizes the need for a holistic approach to ventilation system design, one that integrates airflow dynamics, occupant interaction, and thermal comfort considerations to effectively reduce airborne transmission risks.

## CRediT authorship contribution statement

**Ihab Jabbar Al-Rikabi:** Writing – review & editing, Writing – original draft, Visualization, Methodology, Investigation, Funding acquisition, Formal analysis, Data curation, Conceptualization. **Hayder Alsaad:** Writing – review & editing, Writing – original draft, Visualization, Supervision, Resources, Project administration, Funding acquisition, Conceptualization. **Svenja Carrigan:** Writing – review & editing, Supervision, Resources, Project administration. **Conrad Voelker:** Writing – review & editing, Supervision, Resources, Project administration, Funding acquisition.

## Declaration of competing interest

The authors declare the following financial interests/personal relationships which may be considered as potential competing interests:

Ihab Al-Rikabi reports financial support was provided by Deutscher Akademischer Austaushdienst (DAAD).

## Data availability

No data was used for the research described in the article.

## Acknowledgment

This work was supported by a scholarship from the Deutscher Akademischer Austauschdienst (DAAD) (program ID: 91826206). Their constant support is highly appreciated.

## References

[1] W. Chen, N. Zhang, J. Wei, H.-L. Yen, Y. Li, Short-range airborne route dominates exposure of respiratory infection during close contact, Build. Environ. 176 (2020) 106859, https://doi.org/10.1016/j.buildenv.2020.106859.

[2] K.W. Tham, Indoor air quality and its effects on humans—a review of challenges and developments in the last 30 years, Energy Build. 130 (2016) 637–650, https://doi.org/10.1016/j.enbuild.2016.08.071.

[3] T.T. Moghadam, C.E. Ochoa Morales, M.J. Lopez Zambrano, K. Bruton, D.T.J. O'Sullivan, Energy efficient ventilation and indoor air quality in the context of COVID-19 - a systematic review, Renewable Sustainable Energy Rev. 182 (2023) 113356, https://doi.org/10.1016/j.rser.2023.113356.

[4] Z. Ai, K. Hashimoto, A.K. Melikov, Airborne transmission between room occupants during short-term events: measurement and evaluation, Indoor Air 29 (4) (2019) 563–576, https://doi.org/10.1111/ina.12557.

[5] Z.T. Ai, A.K. Melikov, Airborne spread of expiratory droplet nuclei between the occupants of indoor environments: a review, Indoor Air 28 (4) (2018) 500–524, https://doi.org/10.1111/ina.12465.

[6] B. Yang, A.K. Melikov, A. Kabanshi, C. Zhang, F.S. Bauman, G. Cao, et al., A review of advanced air distribution methods - theory, practice, limitations and solutions, Energy Build. 202 (2019) 109359, https://doi.org/10.1016/j.enbuild.2019.109359.

[7] P.O. Fanger, Introduction of the olf and the decipol units to quantify air pollution perceived by humans indoors and outdoors, Energy Build. 12 (1) (1988) 1–6, https://doi.org/10.1016/0378-7788(88)90051-5.

[8] Z.T. Ai, T. Huang, A.K. Melikov, Airborne transmission of exhaled droplet nuclei between occupants in a room with horizontal air distribution, Build. Environ. 163 (2019) 106328, https://doi.org/10.1016/j.buildenv.2019.106328.

[9] Y. Xie, Z. Ding, J. Ma, X. Zheng, F. Liu, Y. Ding, et al., The assessment of personal exposure in restaurants considering heat sources and ventilation strategies, Energy and Built Environment (2023), https://doi.org/10.1016/j.enbenv.2023.05.005.

[10] J. Cho, Investigation on the contaminant distribution with improved ventilation system in hospital isolation rooms: effect of supply and exhaust air diffuser configurations, Appl. Therm. Eng. 148 (2019) 208–218, https://doi.org/10.1016/j.applthermaleng.2018.11.023.

[11] J. Ye, Z. Ai, Y. Chang, Aerosol transmission in queuing and dining scenarios in canteens and the effectiveness of control measures, Journal of Building Performance Simulation (2023) 1–20, https://doi.org/10.1080/19401493.2023.2193559.

[12] A.K. Melikov, Human body micro-environment: the benefits of controlling airflow interaction, Build. Environ. 91 (2015) 70–77, https://doi.org/10.1016/j.buildenv.2015.04.010.

[13] A. Jurelionis, L. Gagytė, T. Prasauskas, D. Čiužas, E. Krugly, L. Šeduikytė, et al., The impact of the air distribution method in ventilated rooms on the aerosol particle dispersion and removal: the experimental approach, Energy Build. 86 (2015) 305–313, https://doi.org/10.1016/j.enbuild.2014.10.014.

[14] Y. Zhang, G. Cao, G. Feng, K. Xue, C. Pedersen, H.M. Mathisen, et al., The impact of air change rate on the air quality of surgical microenvironment in an operating room with mixing ventilation, J. Build. Eng. 32 (2020) 101770, https://doi.org/10.1016/j.jobe.2020.101770.

[15] K. Xue, G. Cao, M. Liu, Y. Zhang, C. Pedersen, H.M. Mathisen, et al., Experimental study on the effect of exhaust airflows on the surgical environment in an operating room with mixing ventilation, J. Build. Eng. 32 (2020) 101837, https://doi.org/10.1016/j.jobe.2020.101837.
[16] D. Licina, J. Pantelic, A. Melikov, C. Sekhar, K.W. Tham, Experimental investigation of the human convective boundary layer in a quiescent indoor environment, Build. Environ. 75 (2014) 79–91, https://doi.org/10.1016/j.buildenv.2014.01.016.
[17] F.A. Berlanga, I. Olmedo, MR de Adana, J.M. Villafruela, J.S. José, F. Castro, Experimental assessment of different mixing air ventilation systems on ventilation performance and exposure to exhaled contaminants in hospital rooms, Energy Build. 177 (2018) 207–219, https://doi.org/10.1016/j.enbuild.2018.07.053.
[18] S.B. Thool, S.L. Sinha, Performance evaluation of conventional mixing ventilation systems for operating room in the view of infection control by numerical simulation, IJBSBT 6 (4) (2014) 87–98, https://doi.org/10.14257/ijbsbt.2014.6.4.09.
[19] Z. Jiao, S. Yuan, C. Ji, M.S. Mannan, Q. Wang, Optimization of dilution ventilation layout design in confined environments using Computational Fluid Dynamics (CFD), J. Loss Prev. Process. Ind. 60 (2019) 195–202, https://doi.org/10.1016/j.jlp.2019.05.002.
[20] W. Cao, B. Sun, Y. Zhao, Q. Shi, Y. Wang, Study on the transmission route of virus aerosol particles and control technology of air conditioning in the enclosed space, European Physical Journal Plus 136 (10) (2021) 1049, https://doi.org/10.1140/epjp/s13360-021-02058-8.
[21] A. Jurelionis, L. Gagyte, L. Seduikyte, T. Prasauskas, D. Ciuzas, D. Martuzevicius, Combined air heating and ventilation increases risk of personal exposure to airborne pollutants released at the floor level, Energy Build. 116 (2016) 263–273, https://doi.org/10.1016/j.enbuild.2016.01.011.
[22] L. Liu, Y. Li, P.V. Nielsen, J. Wei, R.L. Jensen, Short-range airborne transmission of expiratory droplets between two people, Indoor Air 27 (2) (2017) 452–462, https://doi.org/10.1111/ina.12314.
[23] I. Olmedo, P.V. Nielsen, MR de Adana, R.L. Jensen, The risk of airborne cross-infection in a room with vertical low-velocity ventilation, Indoor Air 23 (1) (2013) 62–73, https://doi.org/10.1111/j.1600-0668.2012.00794.x.
[24] J. Zong, J. Liu, Z. Ai, M.K. Kim, A review of human thermal plume and its influence on the inhalation exposure to particulate matter, Indoor Built Environ. 31 (7) (2022) 1758–1774, https://doi.org/10.1177/1420326X221080358.
[25] P. Peng, M. Pomianowski, C. Zhang, R. Guo, R.L. Jensen, K.T. Jønsson, et al., Experimental investigation on the ventilation performance of diffuse ceiling ventilation in heating conditions, Build. Environ. 205 (2021) 108262, https://doi.org/10.1016/j.buildenv.2021.108262.
[26] J.M. Villafruela, I. Olmedo, J.F. San José, Influence of human breathing modes on airborne cross infection risk, Build. Environ. 106 (2016) 340–351, https://doi.org/10.1016/j.buildenv.2016.07.005.
[27] H. Qian, Y. Li, P.V. Nielsen, C.E. Hyldgaard, T.W. Wong, A.T.Y. Chwang, Dispersion of exhaled droplet nuclei in a two-bed hospital ward with three different ventilation systems, Indoor Air 16 (2) (2006) 111–128, https://doi.org/10.1111/j.1600-0668.2005.00407.x.
[28] I.J. Al-Rikabi, J. Karam, H. Alsaad, K. Ghali, N. Ghaddar, C. Voelker, The impact of mechanical and natural ventilation modes on the spread of indoor airborne contaminants: a review, J. Build. Eng. 85 (2024) 108715, https://doi.org/10.1016/j.jobe.2024.108715.
[29] G. Feng, Y. Bi, Y. Zhang, Y. Cai, K. Huang, Study on the motion law of aerosols produced by human respiration under the action of thermal plume of different intensities, Sustain. Cities Soc. 54 (2020) 101935, https://doi.org/10.1016/j.scs.2019.101935.
[30] I. Olmedo, P.V. Nielsen, M. Ruiz de Adana, R.L. Jensen, P. Grzelecki, Distribution of exhaled contaminants and personal exposure in a room using three different air distribution strategies, Indoor Air 22 (1) (2012) 64–76, https://doi.org/10.1111/j.1600-0668.2011.00736.x.
[31] C. Xu, X. Wei, L. Liu, L. Su, W. Liu, Y. Wang, et al., Effects of personalized ventilation interventions on airborne infection risk and transmission between occupants, Build. Environ. 180 (2020) 107008, https://doi.org/10.1016/j.buildenv.2020.107008.
[32] W. Liu, L. Liu, C. Xu, L. Fu, Y. Wang, P.V. Nielsen, et al., Exploring the potentials of personalized ventilation in mitigating airborne infection risk for two closely ranged occupants with different risk assessment models, Energy Build. 253 (2021) 111531, https://doi.org/10.1016/j.enbuild.2021.111531.
[33] A.K. Melikov, V. Dzhartov, Advanced air distribution for minimizing airborne cross-infection in aircraft cabins, HVAC R Res. 19 (8) (2013) 926–933, https://doi.org/10.1080/10789669.2013.818468.
[34] L. Xiaoping, N. Jianlei, G. Naiping, Spatial distribution of human respiratory droplet residuals and exposure risk for the co-occupant under different ventilation methods, HVAC R Res. 17 (4) (2011) 432–445, https://doi.org/10.1080/10789669.2011.578699.
[35] E. Katramiz, N. Ghaddar, K. Ghali, D. Al-Assaad, S. Ghani, Effect of individually controlled personalized ventilation on cross-contamination due to respiratory activities, Build. Environ. 194 (2021) 107719, https://doi.org/10.1016/j.buildenv.2021.107719.
[36] H. Alsaad, C. Voelker, Performance assessment of a ductless personalized ventilation system using a validated CFD model, Journal of Building Performance Simulation 11 (6) (2018) 689–704, https://doi.org/10.1080/19401493.2018.1431806.
[37] A. Osman, M. Artus, H. Alsaad, C. Koch, C. Voelker, Assessing thermoelectric radiative cooling partition as a personalised comfort system using empirical experiments enhanced by digital shadow visualisation, Build. Environ. (2023) 110833, https://doi.org/10.1016/j.buildenv.2023.110833.
[38] H. Alsaad, C. Voelker, Qualitative evaluation of the flow supplied by personalized ventilation using schlieren imaging and thermography, Build. Environ. 167 (2020) 106450, https://doi.org/10.1016/j.buildenv.2019.106450.
[39] H. Alsaad, C. Voelker, Performance evaluation of ductless personalized ventilation in comparison with desk fans using numerical simulations, Indoor Air 30 (4) (2020) 776–789, https://doi.org/10.1111/ina.12672.
[40] H. Alsaad, C. Voelker, Could the ductless personalized ventilation be an alternative to the regular ducted personalized ventilation? Indoor Air 31 (1) (2021) 99–111, https://doi.org/10.1111/ina.12720.
[41] C. Habchi, K. Ghali, N. Ghaddar, W. Chakroun, S. Alotaibi, Ceiling personalized ventilation combined with desk fans for reduced direct and indirect cross-contamination and efficient use of office space, Energy Convers. Manag. 111 (2016) 158–173, https://doi.org/10.1016/j.enconman.2015.12.067.
[42] C. Xu, P.V. Nielsen, L. Liu, R.L. Jensen, G. Gong, Human exhalation characterization with the aid of schlieren imaging technique, Build. Environ. 112 (2017) 190–199, https://doi.org/10.1016/j.buildenv.2016.11.032.
[43] A. Melikov, J. Kaczmarczyk, Measurement and prediction of indoor air quality using a breathing thermal manikin, Indoor Air 17 (1) (2007) 50–59, https://doi.org/10.1111/j.1600-0668.2006.00451.x.
[44] Z. Ai, C.M. Mak, N. Gao, J. Niu, Tracer gas is a suitable surrogate of exhaled droplet nuclei for studying airborne transmission in the built environment, Build. Simulat. 13 (3) (2020) 489–496, https://doi.org/10.1007/s12273-020-0614-5.
[45] G. Pei, M. Taylor, D. Rim, Human exposure to respiratory aerosols in a ventilated room: effects of ventilation condition, emission mode, and social distancing, Sustain. Cities Soc. 73 (2021) 103090, https://doi.org/10.1016/j.scs.2021.103090.
[46] M. Bivolarova, J. Ondráček, A. Melikov, V. Ždímal, A comparison between tracer gas and aerosol particles distribution indoors: the impact of ventilation rate, interaction of airflows, and presence of objects, Indoor Air 27 (6) (2017) 1201–1212, https://doi.org/10.1111/ina.12388.
[47] I.J. Al-Rikabi, H. Alsaad, P. Nejat, C. Voelker, A comprehensive review on mitigating the risk of airborne particles using add-on systems, Build. Environ. (2023) 110983, https://doi.org/10.1016/j.buildenv.2023.110983.
[48] Z. Liu, T. Wang, Y. Wang, H. Liu, G. Cao, S. Tang, The influence of air supply inlet location on the spatial-temporal distribution of bioaerosol in isolation ward under three mixed ventilation modes, Energy and Built Environment 4 (4) (2023) 445–457, https://doi.org/10.1016/j.enbenv.2022.03.002.
[49] EN 16798-1, Energy performance of buildings - ventilation for buildings - Part 1: indoor environmental input parameters for design and assessment of energy performance of buildings addressing indoor air quality. Thermal Environment, Lighting and Acoustics, first ed., European Committee for Standardization, Switzerland, 2019.
[50] M. Sandberg, What is ventilation efficiency? Build. Environ. 16 (2) (1981) 123–135, https://doi.org/10.1016/0360-1323(81)90028-7.
[51] A. Wang, Y. Zhang, Y. Sun, X. Wang, Experimental study of ventilation effectiveness and air velocity distribution in an aircraft cabin mockup, Build. Environ. 43 (3) (2008) 337–343, https://doi.org/10.1016/j.buildenv.2006.02.024.
[52] D. Rim, A. Novoselac, Ventilation effectiveness as an indicator of occupant exposure to particles from indoor sources, Build. Environ. 45 (5) (2010) 1214–1224, https://doi.org/10.1016/j.buildenv.2009.11.004.
[53] C. Chen, B. Zhao, Some questions on dispersion of human exhaled droplets in ventilation room: answers from numerical investigation, Indoor Air 20 (2) (2010) 95–111, https://doi.org/10.1111/j.1600-0668.2009.00626.x.

[54] S.N. Rudnick, D.K. Milton, Risk of indoor airborne infection transmission estimated from carbon dioxide concentration, Indoor Air 13 (3) (2003) 237–245, https://doi.org/10.1034/j.1600-0668.2003.00189.x.
[55] W.W. Nazaroff, Inhalation intake fraction of pollutants from episodic indoor emissions, Build. Environ. 43 (3) (2008) 269–277, https://doi.org/10.1016/j.buildenv.2006.03.021.
[56] W. Kierat, M. Bivolarova, E. Zavrl, Z. Popiolek, A. Melikov, Accurate assessment of exposure using tracer gas measurements, Build. Environ. 131 (2018) 163–173, https://doi.org/10.1016/j.buildenv.2018.01.017.
[57] E. Katramiz, N. Ghaddar, K. Ghali, Novel personalized chair-ventilation design integrated with displacement ventilation for cross-contamination mitigation in classrooms, Build. Environ. 213 (2022) 108885, https://doi.org/10.1016/j.buildenv.2022.108885.
[58] W.F. Wells, Airborne contagion and air hygiene: an ecological study of droplet infections, JAMA 159 (1) (1955) 90, https://doi.org/10.1001/jama.1955.02960180092033.
[59] E.C. Riley, G. Murphy, R.L. Riley, Airborne spread of measles in a suburban elementary school, Am. J. Epidemiol. 107 (5) (1978) 421–432, https://doi.org/10.1093/oxfordjournals.aje.a112560.
[60] T.-W. Tsang, K.-W. Mui, L.-T. Wong, Computational Fluid Dynamics (CFD) studies on airborne transmission in hospitals: a review on the research approaches and the challenges, J. Build. Eng. 63 (2023) 105533, https://doi.org/10.1016/j.jobe.2022.105533.
[61] Z. Peng, J.L. Jimenez, Exhaled CO2 as a COVID-19 infection risk proxy for different indoor environments and activities, Environ. Sci. Technol. Lett. 8 (5) (2021) 392–397, https://doi.org/10.1021/acs.estlett.1c00183.
[62] S. Zhang, D. Niu, Y. Lu, Z. Lin, Contaminant removal and contaminant dispersion of air distribution for overall and local airborne infection risk controls, Sci. Total Environ. 833 (2022) 155173, https://doi.org/10.1016/j.scitotenv.2022.155173.
[63] Y. Yan, X. Li, X. Fang, Y. Tao, J. Tu, A spatiotemporal assessment of occupants' infection risks in a multi-occupants space using modified Wells-Riley model, Build. Environ. 230 (2023) 110007, https://doi.org/10.1016/j.buildenv.2023.110007.
[64] S. Zhang, Z. Lin, Dilution-based evaluation of airborne infection risk - thorough expansion of Wells-Riley model, Build. Environ. 194 (2021) 107674, https://doi.org/10.1016/j.buildenv.2021.107674.
[65] I.H. Hatif, H. Mohamed Kamar, N. Kamsah, K.Y. Wong, H. Tan, Influence of office furniture on exposure risk to respiratory infection under mixing and displacement air distribution systems, Build. Environ. (2023) 110292, https://doi.org/10.1016/j.buildenv.2023.110292.
[66] X. Liu, Z. Peng, X. Liu, R. Zhou, Dispersion characteristics of hazardous gas and exposure risk assessment in a multiroom building environment, Int. J. Environ. Res. Publ. Health 17 (1) (2019), https://doi.org/10.3390/ijerph17010199.
[67] W. Su, B. Yang, A. Melikov, C. Liang, Y. Lu, F. Wang, et al., Infection probability under different air distribution patterns, Build. Environ. 207 (2022) 108555, https://doi.org/10.1016/j.buildenv.2021.108555.
[68] C. Qin, S.-Z. Zhang, Z.-T. Li, C.-Y. Wen, W.-Z. Lu, Transmission mitigation of COVID-19: exhaled contaminants removal and energy saving in densely occupied space by impinging jet ventilation, Build. Environ. 232 (2023) 110066, https://doi.org/10.1016/j.buildenv.2023.110066.
[69] H. Dai, B. Zhao, Association of the infection probability of COVID-19 with ventilation rates in confined spaces, Build. Simulat. 13 (6) (2020) 1321–1327, https://doi.org/10.1007/s12273-020-0703-5.
[70] Y. Dai, D. Xu, H. Wang, F. Zhang, CFD simulations of ventilation and interunit dispersion in dormitory complex: a case study of epidemic outbreak in Shanghai, Int. J. Environ. Res. Publ. Health 20 (5) (2023), https://doi.org/10.3390/ijerph20054603.
[71] M.K. Fageha, A. Alaidroos, Performance optimization of natural ventilation in classrooms to minimize the probability of viral infection and reduce draught risk, Sustainability 14 (22) (2022) 14966, https://doi.org/10.3390/su142214966.
[72] I.H. Hatif, H.M. Kamar, N. Kamsah, K.Y. Wong, Comparative evaluation of air distribution systems for controlling the airborne infection risk in indoor environments, J. Build. Eng. 79 (2023) 107913, https://doi.org/10.1016/j.jobe.2023.107913.
[73] S. Park, Y. Choi, D. Song, E.K. Kim, Natural ventilation strategy and related issues to prevent coronavirus disease 2019 (COVID-19) airborne transmission in a school building, Sci. Total Environ. 789 (2021) 147764, https://doi.org/10.1016/j.scitotenv.2021.147764.
[74] J. Wei, L. Wang, T. Jin, Y. Li, N. Zhang, Effects of occupant behavior and ventilation on exposure to respiratory droplets in the indoor environment, Build. Environ. 229 (2023) 109973, https://doi.org/10.1016/j.buildenv.2022.109973.